

Silent Hazards of Token Reduction in Vision-Language Models: The Hidden Impact on Consistency

Yizheng Sun¹ Hao Li¹ Chang Xu²
 Chenghua Lin¹ Riza Batista-Navarro¹ Jingyuan Sun^{1,*}
¹University of Manchester ²Microsoft Research
 *Correspondence: jingyuan.sun@manchester.ac.uk

Abstract

Vision-language models (VLMs) have excelled in visual reasoning but often incur high computational costs. One key reason is the redundancy of visual tokens. Although recent token reduction methods claim to achieve minimal performance loss, our extensive experiments reveal that token reduction can substantially alter a model’s output distribution, leading to changes in prediction patterns that standard metrics such as accuracy loss do not fully capture. Such inconsistencies are especially concerning for practical applications where system stability is critical. To investigate this phenomenon, we analyze how token reduction influences the energy distribution of a VLM’s internal representations using a lower-rank approximation via Singular Value Decomposition (SVD). Our results show that changes in the Inverse Participation Ratio of the singular value spectrum are strongly correlated with the model’s consistency after token reduction. Based on these insights, we propose LoFi—a training-free visual token reduction method that utilizes the leverage score from SVD for token pruning. Experimental evaluations demonstrate that LoFi not only reduces computational costs with minimal performance degradation but also significantly outperforms state-of-the-art methods in terms of output consistency.

1. Introduction

Vision-language models (VLMs) have achieved remarkable success by integrating image information as long sequences of visual tokens into large language models [15, 18, 20, 21, 24, 31]. Their ability to reason visually has unlocked applications in various fields, from robotics to multimedia analysis [7, 11, 12, 16]. However, processing these extensive token sequences leads to high computational costs, hindering efficient inference, particularly on edge devices [9, 22, 29, 33]. To overcome this challenge, recent methods have focused on reducing the number of visual tokens

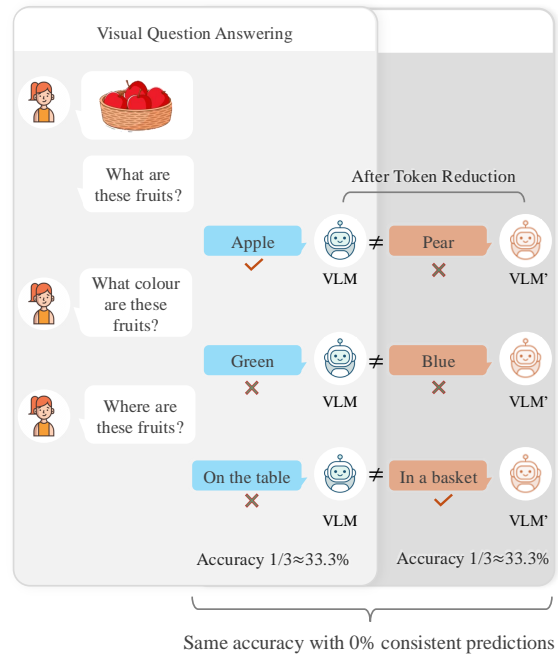


Figure 1. Consider a Visual Question Answering task with three distinct questions. A Vision-Language Model initially answers exactly one correctly ($\sim 33.3\%$ accuracy). After token reduction, the pruned model maintains the same accuracy but answers a different question correctly, resulting in 0% consistency. This demonstrates that identical accuracy fails to capture the significant reasoning divergence caused by token reduction, posing risks for applications requiring reliable and stable outputs.

while preserving task performance. These token reduction approaches are primarily evaluated based on reduced computational cost and minimal losses in benchmark accuracy [25, 26, 28, 30, 32]. This raises an important question: Is token reduction truly benign, or does it introduce changes and influences that standard metrics fail to capture?

One aspect that may be overlooked is the consistency of predictions before and after token reduction. As shown in

Figure 1, consider a visual question answering task where a VLM achieves 33.3% accuracy. After token reduction, the reduced model might be able to achieve a same accuracy with none of the outputs consistent with the original model. Although the overall accuracy remains unchanged, the underlying reasoning has shifted. This inconsistency can be deeply problematic for applications that demand reliable and predictable performance, such as biomedical systems where specific cases must be handled consistently [4, 23]. Our concerns about prediction consistency are validated by extensive experiments in this paper. We evaluate multiple popular token reduction methods [25, 28, 32] on various visual question answering benchmarks [8, 10, 27]. Although these methods claim impressively high accuracy after token reduction, our findings reveal significant discrepancies in prediction patterns between the original VLM and its token-reduced counterparts. These discrepancies underscore the critical importance of measuring consistency, driving our focus on consistency preservation throughout this study.

To understand these inconsistencies, we hypothesize that shifts in the model’s internal representations are responsible for the changes in final predictions. We examine this by assessing how token reduction disrupts the energy distribution within the internal representations. Specifically, we apply truncated Singular Value Decomposition (SVD) [3] to the attention output matrices at each transformer layer. SVD identifies the principal directions—those components that capture the most energy of the underlying structure. We then validate whether token reduction disrupts this structure by observing changes in the distribution of these principal directions. For this purpose, we use the Inverse Participation Ratio (IPR) [2] of the singular value spectrum as a key indicator. A lower IPR suggests that energy is more evenly spread across components, whereas a higher IPR indicates that energy is concentrated in fewer components. By quantifying the change in IPR for each layer following token reduction, we observe a strong correlation with the output consistency between the pruned and original models. In other words, when the IPR scores remain relatively stable after token reduction, the pruned model’s outputs tend to align closely with those of the original model, and vice versa.

Building upon these insights, we propose a novel training-free token reduction method that preserves model fidelity by minimising its disruption on a VLM’s internal representations. Our approach leverages internal statistics from the truncated SVD. By computing leverage scores from the truncated right singular vectors [6], we can quantify each token’s contribution to the dominant subspace, allowing us to dynamically prune tokens. By selectively removing these less influential tokens, our method leads to high consistency with the original VLM’s outputs and retains accuracy while significantly reducing computational

costs, as supported by comprehensive experimental results. In summary, our work makes the following contributions:

- We reveal that token reduction for VLMs can lead to significant output inconsistencies, despite retaining high benchmark accuracy, highlighting potential risks in applications requiring stable outputs.
- We propose a truncated SVD and IPR-based metric to assess layer-wise token reduction effects, revealing a strong correlation with output consistency.
- We introduce a training-free strategy that lowers computational cost while preserving model fidelity, improving both efficiency and stability across multiple benchmarks.

2. Related Works

2.1. Vision-Language Models (VLMs)

Recent advancements in multimodal large language models (MLLMs) have significantly improved the integration of visual and textual information. BLIP [13] pioneered unified vision-language pretraining with bootstrapped captions. BLIP-2 [14] introduced a two-stage framework that links pre-trained vision models with language models using a Q-former as a vision encoder, thereby generating a condensed set of vision tokens for efficient processing. Building on this approach, InstructBLIP [5] incorporated instruction tuning to enable more complex prompts and support a wider range of tasks. More recent VLMs aim to scale multimodal capabilities even further, Qwen [1], for example, achieved state-of-the-art performance among open-source models. Meanwhile, LLaVA series models [17, 19, 21] proposed to process long sequences of vision tokens without compression, demonstrating strong performance and data efficiency. However, this uncompressed approach incurs a substantial computational cost, illustrating the trade-off between computational efficiency and overall performance.

2.2. Token Reduction for VLMs

In Vision-Language Models (VLMs), token reduction is a technique designed to improve efficiency by reducing the number of tokens that the model processes. LLaVA-PruMerge adaptively selected and merged vision tokens based on attention scores, ensuring that pruned token information is preserved within retained tokens [25]. TRIM, in contrast, leveraged a CLIP-based similarity metric to identify vision tokens most relevant to a given text prompt, making it more query-dependent [28]. VisionZip took a text-agnostic approach by selecting dominant tokens with high attention values while merging remaining tokens into contextual representations [32]. Although these methods reported impressively low benchmark performance loss, they largely overlook output consistency, which measures how the token reduced models’ outputs aligned with their full-token counterparts. This gap motivates our investigation

into output consistency in token-reduced VLMs.

3. Methodology

To address the issue of low output consistency, we first look into what is causing it. We analyze this by measuring how energy distribution of internal representations change after token reduction. We conduct low rank approximation through SVD, which extracts the most informative components of a model’s internal representations in principal directions. In this way, we investigate whether token reduction disrupts the principal directions of internal representations across different layers in the VLM.

As detailed in Section 3.1, we introduce a layer-wise metric with truncated SVD to measure the difference between the energy distributions of the reduced model and the original model, quantifying disruptions in internal representations. The effectiveness of this metric is supported by the experimental results in Figure 3 and will be discussed in detail in Section 5.2. Next, guided by this metric, we aim to minimize disruptions to internal representations caused by token reduction to alleviate the consistency issue. Based on this principle, we propose LoFi in Section 3.2, a token reduction method that does not require extra training and aims for minimal performance loss while keeping output consistency high.

3.1. LID: Layer-wise Internal Disruption Metric

To precisely quantify how token reduction disrupts the principal directions of internal representations across model layers, we require a consistent measurement of disruption. A key challenge arises from the mismatch in dimensions between internal representations of the original and token-reduced models, as token pruning directly alters token count and consequently internal representation dimensions. Direct comparisons of internal representations or attention matrices are thus impractical due to this dimensionality mismatch. To overcome this challenge, we propose the Layer-wise Internal Disruption (LID) metric. LID quantifies the distribution of principal directions in internal representations and is robust to differences in matrix shapes caused by token pruning.

3.1.1. Formal Definition

We now formally define the Layer-wise Internal Disruption metric using Singular Value Decomposition (SVD) and the Inverse Participation Ratio (IPR). First, consider the general architecture of vision-language models illustrated in Figure 2. A VLM typically consists of stacked transformer layers, each processing unified token sequences comprising both visual and textual tokens. At each transformer layer, we perform truncated SVD on the attention output matrix to capture its principal directions. We then compute the IPR to measure how concentrated the energy is across these princi-

pal directions, effectively characterizing the distribution of internal representation energies. Changes in IPR values between the original and reduced models directly reflect disruptions introduced by token pruning. Below, we introduce the necessary background on SVD and IPR in detail.

SVD Factorization. We begin by taking the attention output $O \in \mathbb{R}^{D \times N}$ from a given layer in the VLM, where N is the number of tokens and D is the embedding dimension. We use SVD to factorize the attention output matrix O . SVD decomposes a matrix into singular values and singular vectors. In many cases, most of the important information, or the most significant principle directions of O is captured by the largest singular values and their corresponding vectors. We therefore form a truncated SVD with rank r by keeping only the top- r singular values and the corresponding singular vectors. Specifically, we approximate O as:

$$O \approx U_r \Sigma_r V_r^T. \quad (1)$$

Here, r is a constant, $U_r \in \mathbb{R}^{D \times r}$ contains the top r left singular vectors, $\Sigma_r \in \mathbb{R}^{r \times r}$ is a diagonal matrix with the top r singular values, and $V_r \in \mathbb{R}^{N \times r}$ contains the top r right singular vectors. This decomposition captures the top- r principal directions of O , allowing us to focus on the most significant principle directions. In all our experiments, we set $r = \lfloor \frac{3}{4}r \rfloor$ by default, unless stated otherwise.

Inverse Participation Ratio (IPR). Truncated SVD identifies principal directions in O , corresponding to its most informative components. We can analyze how these directions are distributed, especially in terms of how sparse or concentrated they are. Such analysis will provide clear insights about how the components that are most critical for representing the underlying structure of O are distributed. Then, whether token reduction disrupts the structure of internal representations can be validated by observing whether it influences the distribution of principle directions. The Inverse Participation Ratio (IPR) is a metric used to assess the degree of localization of data [2]. Measuring the difference of IPR on the singular value matrix before and after token reduction can quantify the disruption in internal representations caused by token reduction across layers. Specifically, we define $\{\sigma_i\}$ as the singular values in Σ_r ,

$$\text{IPR}(\{\sigma_i\}) = \frac{\sum_{i=1}^r \sigma_i^4}{\left(\sum_{i=1}^r \sigma_i^2\right)^2}. \quad (2)$$

As shown in Figure 2, the denominator $(\sum_{i=1}^r \sigma_i^2)^2$ represents the overall magnitude of all principal directions in the internal representations. The numerator $(\sum_{i=1}^r \sigma_i^4)$ emphasizes those with larger magnitudes by raising them to the fourth power. Thus, a higher IPR indicates an uneven

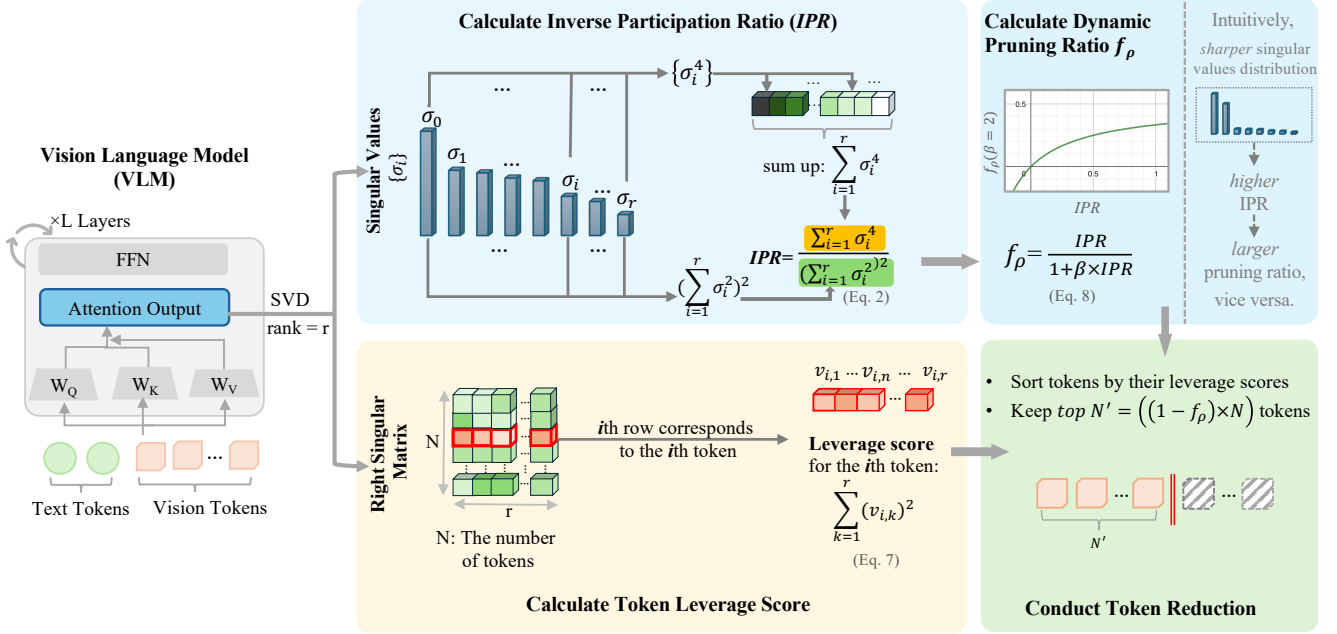


Figure 2. **LoFi Framework Overview**: For each layer in a VLM, truncated SVD factorizes the attention output into low-rank matrices. First, we compute the Inverse Participation Ratio (IPR) from the singular values. Concurrently, we derive token leverage scores from the right singular matrix to measure each token’s contribution to the top- r principal directions. Next, we determine a dynamic pruning ratio using a monotonically increasing function on $[0, 1]$. Finally, we retain the tokens with the highest leverage scores based on this ratio.

distribution of the principle directions, with a few directions dominating significantly, whereas a lower IPR indicates a more uniform distribution of directions. In this way, IPR effectively quantifies the principle directions distribution of a layer’s internal representation.

Layer-wise Combination As the IPR quantifies the distribution of principal directions within each individual layer’s internal representation, we aggregate these layer-wise IPR values into a unified vector to effectively capture the overall disruption caused by token reduction. Formally, we define f_{original} as the original VLM and f_{reduced} as its token-reduced counterpart, where each model consists of L transformer layers. For a given layer x , we represent its contribution to this aggregated measure as follows:

$$\text{ipr}_{\text{original}}^x = \text{IPR}(\{\sigma_i^x\}), \quad \text{ipr}_{\text{reduced}}^x = \text{IPR}(\{\hat{\sigma}_i^x\}), \quad (3)$$

where $\{\sigma_i^x\}$ are layer- x singular values for f_{original} , and $\{\hat{\sigma}_i^x\}$ are those for f_{reduced} . We gather these into:

$$\ell_{\text{original}} = [\text{ipr}_{\text{original}}^1, \dots, \text{ipr}_{\text{original}}^L], \quad (4)$$

$$\ell_{\text{reduced}} = [\text{ipr}_{\text{reduced}}^1, \dots, \text{ipr}_{\text{reduced}}^L]. \quad (5)$$

Intuitively, ℓ_{original} and ℓ_{reduced} represent the overall distributions of principal directions in internal representations for the original VLM and its token-reduced counterpart, respectively. The distance between these two vectors represent the

disruption caused by token reduction. To quantify this disruption, we propose a Layer-wise Internal Disruption Metric (LID), which is the L1 norm distance between ℓ_{original} and ℓ_{reduced} . Specifically, we define:

$$\text{LID}(\ell_{\text{original}}, \ell_{\text{reduced}}) = \sum_{i=1}^L |\text{ipr}_{\text{original}}^i - \text{ipr}_{\text{reduced}}^i|. \quad (6)$$

3.2. LoFi: Low Rank Token Filtering

LID offers a means to quantify the disruption caused by token reduction in the internal representations for a VLM. We also find that LID is strongly linearly correlated with output consistency which will be detailed in Section 5.2. This suggests that disruptions in internal representations are a key factor behind low consistency. Hence, minimizing LID should be promising in improving output consistency. To address this, we introduce LoFi (LOW Rank Token Filtering), whose architecture is illustrated in Figure 2. LoFi reduces LID through two main innovations: Leverage Score and Dynamic Pruning Ratio, which will be described in Section 3.2.1 and 3.2.2. Then in Section 3.2.3, we introduce how to conduct token reduction based on Leverage Score with Dynamic Pruning Ratio.

3.2.1. Token Leverage Score

To minimize LID, we need to minimize the token reduction’s disruption on the principal distribution in a VLM’s

internal representations. To this end, the intuitive idea is to remove the tokens that have the least importance, and we need to measure the importance of tokens. In previous steps, we have conducted truncated SVD attention output matrices for low rank approximation. In this context, leverage score, a linear algebra metric that measures the contribution of a data point in representing the dominant, low-rank structure of a matrix will be an ideal choice to take. It quantifies the extent to which that point is represented in the principal directions, reflecting its importance.

Specifically, as shown in Figure 2, let the attention output matrix O have shape $D \times N$, where N is the number of tokens. By applying truncated SVD with rank r on O , we obtain the right singular matrix V_r . Each row of V_r corresponds to the representation of a column vector from O in the low-rank subspace, which corresponds indirectly to a token. The leverage score for the i th token is defined as follows:

$$\mathcal{S}_i = \|(V_r)_{i,:}\|^2 = \sum_{k=1}^r (V_r)_{i,k}^2, \quad i = 1, \dots, N. \quad (7)$$

Intuitively, a high leverage score \mathcal{S}_i for a token indicates that it has a strong representation in the top- r subspace of O . This means the token contributes significantly to the overall structure of O . Such tokens are considered important and should be retained. Conversely, a low leverage score means that the token does not contribute much to the dominant structure of O . These tokens are less important and can be removed or merged during our token reduction process.

3.2.2. Dynamic Pruning Ratio.

When conducting token reduction, an important decision is determining the ratio of tokens to prune. We propose a dynamic pruning ratio. The motivation for using a dynamic rather than a fixed ratio comes from our observation that the IPR value differs significantly across layers, indicating that the principal direction distribution varies. In layers where the internal representation exhibits a relatively uniform distribution—meaning each principal direction holds considerable significance—pruning too many tokens would lead to greater disruptions. Thus, a fixed pruning ratio is intuitively inadequate. Given that the IPR value effectively reflects the principal direction distribution within a layer, we propose a dynamic pruning ratio, f_ρ , which is determined by the IPR value at each layer. Specifically:

$$f_\rho = \frac{\text{IPR}(\sigma_i)}{1 + \beta \text{IPR}(\sigma_i)}. \quad (8)$$

Here, β is a positive hyper-parameter that controls the aggressiveness of token reduction—a smaller β yields a higher pruning ratio, and vice versa. As illustrated in Figure 2, a higher IPR corresponds to a greater concentration among the principal directions, implying that more tokens

can be removed and thus a higher value of f_ρ . We will detail the benefits of using this dynamic pruning ratio in Section 5.4 of Experimental Results.

3.2.3. Token Reduction Procedure

Finally, we describe the steps of how LoFi uses token leverage score to reduce the number of tokens with dynamic pruning ratio. We sort tokens by their leverage scores \mathcal{S}_i in descending order:

$$\ell_1 \geq \ell_2 \geq \dots \geq \ell_N. \quad (9)$$

Given a pruning ratio f_ρ , we remove the bottom $R = \lfloor f_\rho \times N \rfloor$ tokens in this sorted list, i.e., those with the smallest leverage scores. All the aforementioned tokens are vision tokens.

To preserve pruned tokens’ information, we merge their embeddings into a single vector. Let

$$\mathcal{P} = \{e_i \mid i \in \mathcal{I}_{\text{pruned}}\} \quad (10)$$

be the set of pruned token embeddings, where each $e_i \in \mathbb{R}^D$. Because pruned tokens have different leverage scores. We merge them with weights based on their leverage scores. Specifically, defining ℓ_i as the leverage score of token i , we calculate its merging weight by normalizing its leverage score:

$$w_i = \frac{\ell_i}{\sum_{j \in \mathcal{I}_{\text{pruned}}} \ell_j}, \quad i \in \mathcal{I}_{\text{pruned}}. \quad (11)$$

Then, we compute a weighted merged embedding:

$$e_{\text{merged}} = \sum_{i \in \mathcal{I}_{\text{pruned}}} w_i e_i. \quad (12)$$

We place e_{merged} in the middle of the pruned tokens’ positions (using the median index of $\mathcal{I}_{\text{pruned}}$), thereby retaining their collective information in a single embedding.

4. Experimental Setup

Datasets We evaluate our method using three widely-adopted open-ended visual question answering (VQA) datasets: GQA [10], VQAv2 [8], and TextVQA [27]. These datasets are selected for their short, free-form answers (typically one word or a brief phrase) and broad domain coverage, making them particularly suitable for assessing output consistency. We primarily utilize GQA and VQAv2 due to their extensive scale and diverse question domains. TextVQA serves as a supplementary benchmark due to its smaller scale and specific focus on text recognition within images.

Baselines We select three representative token reduction methods. LLava-Prumerge+ reduces tokens by compressing visual tokens based on their similarity to the class token [25]. TRIM reduces the number of vision tokens by

Method	Setting	GQA			VQAv2			TextVQA			AVG Accuracy (%)↑	AVG Consistency (%)↑	AVG TFLOps (%)↓
		Accuracy (%)↑	Consistency (%)↑	AVG TFLOps per sample↓	Accuracy (%)↑	Consistency (%)↑	AVG TFLOps per sample↓	Accuracy (%)↑	Consistency (%)↑	AVG TFLOps per sample↓			
Vanilla LLaVA-1.5	--	62	--	9.04	78.53	--	9	58.21	--	9.80	66.25	--	9.28
Prumerge+	Finetuned	59.37 →95.76%	80.23	3.13 ↓65.38%	76.86 →97.87%	81.21	3.1 ↓65.56%	56.01* →96.22%	68.76	4.21 ↓57.04%	64.08	76.73	3.48
	w/o Finetune	57.39 →92.56%	80.76	3.13 ↓65.38%	74.64 →95.05%	82.42	3.1 ↓65.56%	54.95 →94.40%	75.71	4.21 ↓57.04%	62.33	79.63	3.48
TRIM	Finetuned	61.42 →99.06%	80.08	2.82 ↓68.81%	76.64* →97.59%	80.27	2.78 ↓69.11%	53.16* →91.32%	65.36	3.57 ↓63.57%	63.74	75.24	3.06
	w/o Finetune	58.75 →94.76%	81.73	2.82 ↓68.81%	76.29 →97.15%	81.91	2.78 ↓69.11%	52.57 →90.31%	69.74	3.57 ↓63.57%	62.54	77.79	3.06
VisionZip	Retain 192 tokens	59.22 →95.52%	85.57	3.73 ↓58.74%	76.77 →97.76%	87.57	3.7 ↓58.89%	57.25 →98.35%	82	4.47 ↓54.39%	64.41	85.05	3.97
	Retain 128 tokens	57.62 →92.94%	81.28	2.89 ↓68.03%	75.6 →96.27%	84.47	2.85 ↓68.33%	56.85 →97.66%	79.52	3.62 ↓63.06%	63.36	81.76	3.12
	Retain 64 tokens	55.13 →88.92%	75.63	2.04 ↓77.43%	72.41 →92.21%	78.1	2 ↓77.78%	55.52 →95.38%	73.66	2.78 ↓71.63%	61.02	75.8	2.27
LOFI	$\beta = 6$	61.19 →98.6%	88.96	3.89 ↓56.97%	76.62 →97.57%	87.93	3.81 ↓57.67%	56.56 →97.17%	81.72	4.77 ↓51.33%	64.79	86.2	4.16
	$\beta = 4$	60.76 →97.74%	87.26	3.48 ↓61.50%	76.17 →96.99%	86.24	3.4 ↓62.22%	56.35 →96.8%	81.02	4.36 ↓55.51%	64.43	84.84	3.75
	$\beta = 2$	59.65 →96.21%	84.75	2.98 ↓67.04%	74.88 →95.35%	83.56	2.91 ↓67.67%	55.8 →95.86%	78.86	3.87 ↓60.51%	63.44	82.39	3.25

Table 1. **Evaluation results comparing LLaVA-Prumerge [25], TRIM [28], VisionZip [32], and LOFI (ours).** We apply the token reduction methods to LLaVA-1.5 [20] model. The first row provides baseline accuracy and average TFLOPs per sample for LLaVA-1.5 without token reduction. For each method, we separately report accuracy, consistency, and TFLOPs on the GQA, VQAv2, and TextVQA benchmarks. The last three columns show average performance metrics computed across these three benchmarks. The right arrow (\rightarrow) represents the percentage of accuracy retained, and the down arrow (\downarrow) represents the percentage of TFLOPs reduced. *Using official codebases, we observed minor differences in results compared to those reported in the original papers under our experiments environment.

leveraging the similarity between text tokens and vision tokens [28]. VisionZip focuses on selecting the most informative visual tokens from the encoder output [32]. We adopt the LLaVA-1.5 [20] model as the target Vision-Language Model (VLM) for applying our token reduction methods.

Metrics The metrics we report are three-fold. Firstly, we report Accuracy to measure the percentage of questions answered correctly. Secondly, we use output consistency to quantify the fraction of answers where the pruned model agrees with the original model’s output. Specifically, we define an output pair $out_i = (out_i^{reduce}, out_i^{original})$ as the combination of the outputs from the pruned model and the original model for the i th input. We define the consistency value as follows:

$$\text{consistency} = \frac{\text{size}(\{out_k | k \in \mathcal{I}_{\text{different}}\})}{S},$$

where $\mathcal{I}_{\text{different}}$ is the set of indices for all output pairs that have different entries, S is the number of all output pairs. Finally, we report forward average TFLOPs, which demonstrates the average per-input computational cost in tera-floating-point operations [34].

Method	GQA		VQAv2	
	Layer-wise Inner Disruption (LID)	Consistency (%)	Layer-wise Inner Disruption (LID)	Consistency (%)
Prumerge+	2.24	80.76	2.26	82.42
Prumerge+(Finetune)	2.29	80.23	2.27	81.21
TRIM	2.01	81.73	2.00	81.91
TRIM(Finetune)	2.25	80.08	2.19	80.27
Visionzip 192	1.67	85.57	1.74	87.57
Visionzip 128	2.09	81.28	2.16	84.47
Visionzip 64	2.73	75.63	2.81	78.10
LOFI ($\beta=6$)	1.26	88.96	1.37	87.93
LOFI ($\beta=4$)	1.56	87.26	1.67	86.24
LOFI ($\beta=2$)	2.00	84.75	2.13	83.56
Pearson correlation \mathcal{R}	-0.978		-0.908	

Table 2. **Layer-wise Internal Disruption Metric (LID) and output consistency results on GQA [10] and VQAv2 [8].** Pearson correlation \mathcal{R} measures the strength and direction of a linear relationship between LID and Consistency.

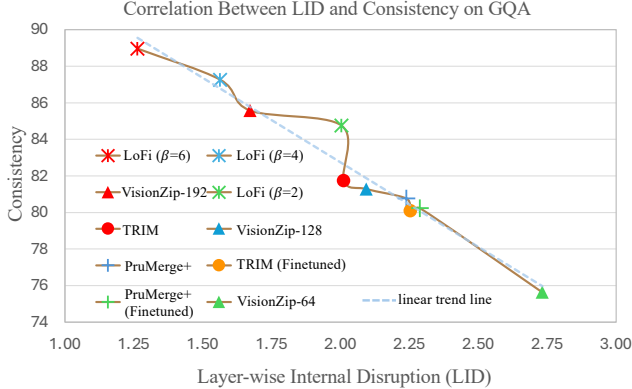


Figure 3. Correlation between the proposed Layer-wise Internal Disruption (LID) and output consistency on GQA [10].

5. Experimental Results

We first evaluate several existing token reduction methods to examine consistency issues (Section 5.1). Next, we assess whether disruptions in internal representations cause these issues by evaluating the Layer-wise Inner Disruption (LID) metric (Section 5.2). We then demonstrate that our LoFi method reduces computational costs without compromising performance or consistency (Section 5.3). An ablation study comparing dynamic and fixed pruning ratios is also conducted (Section 5.4), and finally, we test the generalization of LoFi on the LLaVA-NEXT [21] model (Section 5.5).

5.1. Consistency Analysis for Existing Token Reduction Methods

Our goal in this experiment is to determine whether current token reduction methods suffer from low consistency and to quantify the issue. We conduct experiments using Prumerge+, TRIM, and VisionZip on the GQA, VQAv2, and TextVQA benchmarks. As shown in Table 1, there is a significant gap between accuracy preservation and consistency. For instance, while Prumerge+ achieves over 95% accuracy on VQAv2, GQA, and other benchmarks, its consistency drops to around 80% for VQAv2 and GQA, and to approximately 69% in some cases. TRIM also maintains high accuracy but shows similar consistency issues. VisionZip performs slightly better, with consistency values of about 87% on VQAv2 and 85% on GQA, alongside roughly 95% accuracy. This gap highlights a critical limitation: current methods prioritize accuracy over consistency.

5.2. Effectiveness Analysis for Layer-wise Internal Disruption (LID)

As discussed in Section 3.1, disruptions in internal representations within model layers are hypothesized as a primary cause of low consistency. To test this hypothesis, we

investigate whether our proposed Layer-wise Inner Disruption (LID) metric correlates with consistency scores. We conduct experiments measuring LID and consistency for various token reduction methods, with detailed results in Table 2. To quantify the correlation, we compute the Pearson correlation coefficient. Given pairs (x_i, y_i) representing LID and consistency values, respectively, the Pearson coefficient \mathcal{R} is defined as:

$$\mathcal{R} = \frac{\sum_{i=1}^n (x_i - \bar{x})(y_i - \bar{y})}{\sqrt{\sum_{i=1}^n (x_i - \bar{x})^2} \sqrt{\sum_{i=1}^n (y_i - \bar{y})^2}},$$

where n is the number of data points, and \bar{x} , \bar{y} represent the mean values of all x_i values and y_i values, respectively. Table 2 shows that the Pearson coefficients are strongly negative—approximately -0.978 for GQA and -0.908 for VQAv2. Figure 3 further illustrates that as LID values increase, consistency values decrease across all evaluated methods. These findings confirm that the LID metric effectively captures internal representation disruptions, strongly supporting our hypothesis that layer disruption significantly contributes to the observed low consistency issue.

5.3. Effectiveness Analysis of LoFi

We conduct extensive evaluations on three benchmarks to validate LoFi’s ability to maintain high accuracy and consistency simultaneously. We test three hyperparameter settings ($\beta = 2, 4, 6$), each corresponding to a different level of computational cost reduction. Table 1 summarizes the trade-offs between accuracy, consistency, and computational efficiency (measured in TFLOPs) across all methods.

Notably, LoFi consistently outperforms baseline methods in maintaining higher consistency. For instance, at comparable TFLOP reductions (about 60%–70%), LoFi achieves a consistency score of approximately 88.9% on GQA, whereas Prumerge+ reaches around 80%, TRIM attains a maximum of 81.7%, and VisionZip ranges between 75.6% and 85.6%. Additionally, LoFi maintains competitive accuracy, scoring 76.6% on the VQAv2 benchmark. Although LoFi’s consistency slightly declines under more aggressive reductions on benchmarks like VQAv2, it still outperforms other methods. Overall, averaging accuracy and consistency across all benchmarks demonstrates that LoFi with $\beta = 6$ consistently delivers superior performance, effectively balancing both metrics.

5.4. Ablation Study: Dynamic Pruning Ratio

To show the benefits of a dynamic pruning ratio over fixed ratios, as discussed in Section 3.2.3, we compare the dynamic approach against two fixed ratios ($\theta = 0.9$ and $\theta = 0.85$), where θ denotes the fraction of retained vision tokens. We use the dynamic strategy with $\beta = 4$ as our example setting. As shown in Table 3, dynamic pruning consistently achieves higher accuracy and output consistency

Pruning Ratio Type	GQA			VQAv2			TextVQA		
	Accuracy (%) \uparrow	Consistency (%) \uparrow	AVG TFlops per sample \downarrow	Accuracy (%) \uparrow	Consistency (%) \uparrow	AVG TFlops per sample \downarrow	Accuracy (%) \uparrow	Consistency (%) \uparrow	AVG TFlops per sample \downarrow
Dynamic pruning ratio $\beta=4$	60.76	87.26	3.48	76.17	86.24	3.4	56.35	81.02	4.36
Fixed pruning ratio $\theta=0.9$	60.07	85.88	3.65	75.75	85.97	3.61	55.34	78.78	4.38
Fixed pruning ratio $\theta=0.85$	59.22	82.39	3.02	73.73	81.01	2.98	53.96	73.28	3.75

Table 3. **Ablation study on dynamic vs. fixed pruning ratios.** We compare our dynamic pruning strategy (with $\beta = 4$) against two fixed pruning ratios ($\theta = 0.9, 0.85$), corresponding to pruning 10% and 15% of vision tokens per layer, respectively.

	GQA			VQAv2			TextVQA		
	Accuracy (%) \uparrow	Consistency (%) \uparrow	AVG TFlops per sample \downarrow	Accuracy (%) \uparrow	Consistency (%) \uparrow	AVG TFlops per sample \downarrow	Accuracy (%) \uparrow	Consistency (%) \uparrow	AVG TFlops per sample \downarrow
Vanilla LLaVA-Next	64.25	--	34.75	81.83	--	34.9	61.39	--	37.3
LoFi ($\beta=4$)	61.93 \rightarrow 96.39%	84.83	10.42 \downarrow 70.01%	78.81 \rightarrow 96.31%	86.11	10.11 \downarrow 71.03%	57.04 \rightarrow 92.91%	79.4	11.16 \downarrow 68.9%

Table 4. **LoFi results on LLaVA-NEXT [21].** We evaluate LoFi using $\beta = 4$ as a representative configuration. Compared to its application on LLaVA-1.5, LoFi applied to LLaVA-NEXT achieves significantly greater computational cost reductions while maintaining high accuracy and consistency.

across GQA, VQAv2, and TextVQA at comparable or lower computational costs (TFLOPs). For instance, on GQA, dynamic pruning attains 87.3% consistency and 60.8% accuracy, compared to fixed ratios that reach at most 85.9% consistency and 60.1% accuracy. Similar trends are observed in VQAv2 and TextVQA. These results confirm that dynamically adjusting the pruning ratio effectively preserves both accuracy and consistency while maintaining computational efficiency.

5.5. Applying LoFi to LLaVA-NEXT

In order to evaluate the generalization capability of LoFi, we test whether it addresses the consistency issue across different model architectures. We apply LoFi to the LLaVA-Next model using a representative setting of $\beta = 4$. As shown in Table 4, LoFi achieves approximately 85% consistency on GQA and 86% on VQAv2 while preserving over 96% accuracy. Notably, compared to LLaVA-1.5 under the same hyper-parameter setting, LoFi reduces computational cost by about 70% in FLOPs. This result indicates that vision tokens in LLaVA-Next are more redundant than those in LLaVA-1.5, and LoFi effectively adapts by dynamically adjusting the number of vision tokens.

6. Conclusion

This work addresses the previously overlooked issue of output consistency in token reduction for Vision-Language Models (VLMs). We introduce the Layer-wise Internal Disruption (LID) metric, demonstrating that disruptions to in-

ternal layer representations caused by token reduction significantly contribute to reduced output consistency. Building upon this insight, we propose LoFi, a training-free approach designed to maintain model fidelity by minimizing these internal disruptions. Experimental results confirm that LoFi consistently outperforms existing methods in terms of both output consistency and computational efficiency. Our findings highlight the importance of consistency-aware token pruning and provide a foundation for developing adaptive strategies in future research.

References

- [1] Jinze Bai, Shuai Bai, Shusheng Yang, Shijie Wang, Sinan Tan, Peng Wang, Junyang Lin, Chang Zhou, and Jingren Zhou. Qwen-vl: A frontier large vision-language model with versatile abilities. *CoRR*, abs/2308.12966, 2023. 2
- [2] R. J. Bell and P. Dean. Atomic vibrations in vitreous silica. *Discussions of the Faraday Society*, 50:55–61, 1970. 2, 3
- [3] Tony F. Chan and Per Christian Hansen. Computing truncated singular value decomposition least squares solutions by rank revealing qr-factorizations. *SIAM J. Sci. Comput.*, 11(3):519–530, 1990. 2
- [4] Evangelia Christodoulou, Annika Reinke, Rola Houhou, Piotr Kalinowski, Selen Erkan, Carole H. Sudre, Ninon Burgos, Sofiène Boutaj, Sophie Loizillon, Maëlys Solal, Nicola Rieke, Veronika Cheplygina, Michela Antonelli, Leon D. Mayer, Minu Dietlinde Tizabi, M. Jorge Cardoso, Amber L. Simpson, Paul F. Jäger, Annette Kopp-Schneider, Gaël Varoquaux, Olivier Colliot, and Lena Maier-Hein. Confidence intervals uncovered: Are we ready for real-world medical

- imaging ai? In *MICCAI (10)*, pages 124–132. Springer, 2024. 2
- [5] Wenliang Dai, Junnan Li, Dongxu Li, Anthony Meng Huat Tiong, Junqi Zhao, Weisheng Wang, Boyang Li, Pascale Fung, and Steven C. H. Hoi. Instructblip: Towards general-purpose vision-language models with instruction tuning. In *NeurIPS*, 2023. 2
- [6] Petros Drineas, Michael W. Mahoney, and S. Muthukrishnan. Relative-error CUR matrix decompositions. *SIAM J. Matrix Anal. Appl.*, 30(2):844–881, 2008. 2
- [7] Rohit Girdhar, Alaaeldin El-Nouby, Zhuang Liu, Mannat Singh, Kalyan Vasudev Alwala, Armand Joulin, and Ishan Misra. Imagebind one embedding space to bind them all. In *CVPR*, pages 15180–15190. IEEE, 2023. 1
- [8] Yash Goyal, Tejas Khot, Aishwarya Agrawal, Douglas Summers-Stay, Dhruv Batra, and Devi Parikh. Making the V in VQA matter: Elevating the role of image understanding in visual question answering. *Int. J. Comput. Vis.*, 127(4):398–414, 2019. 2, 5, 6
- [9] Jude Haris, Rappy Saha, Wenhao Hu, and José Cano. Designing efficient LLM accelerators for edge devices. *CoRR*, abs/2408.00462, 2024. 1
- [10] Drew A. Hudson and Christopher D. Manning. GQA: A new dataset for real-world visual reasoning and compositional question answering. In *CVPR*, pages 6700–6709. Computer Vision Foundation / IEEE, 2019. 2, 5, 6, 7
- [11] Brian Ichter, Anthony Brohan, Yevgen Chebotar, Chelsea Finn, Karol Hausman, Alexander Herzog, Daniel Ho, Julian Ibarz, Alex Irpan, Eric Jang, Ryan Julian, Dmitry Kalashnikov, Sergey Levine, Yao Lu, Carolina Parada, Kanishk Rao, Pierre Sermanet, Alexander Toshev, Vincent Vanhoucke, Fei Xia, Ted Xiao, Peng Xu, Mengyuan Yan, Noah Brown, Michael Ahn, Omar Cortes, Nicolas Sievers, Clayton Tan, Sichun Xu, Diego Reyes, Jarek Rettinghouse, Jor-nell Quiambao, Peter Pastor, Linda Luu, Kuang-Huei Lee, Yuheng Kuang, Sally Jesmonth, Nikhil J. Joshi, Kyle Jeffrey, Rosario Jauregui Ruano, Jasmine Hsu, Keerthana Gopalakrishnan, Byron David, Andy Zeng, and Chuyuan Kelly Fu. Do as I can, not as I say: Grounding language in robotic affordances. In *CoRL*, pages 287–318. PMLR, 2022. 1
- [12] Hao Li, Yu-Hao Huang, Chang Xu, Viktor Schlegel, Ren-He Jiang, Riza Batista-Navarro, Goran Nenadic, and Jiang Bian. Bridge: Bootstrapping text to control time-series generation via multi-agent iterative optimization and diffusion modelling. *arXiv preprint arXiv:2503.02445*, 2025. 1
- [13] Junnan Li, Dongxu Li, Caiming Xiong, and Steven C. H. Hoi. BLIP: bootstrapping language-image pre-training for unified vision-language understanding and generation. In *ICML*, pages 12888–12900. PMLR, 2022. 2
- [14] Junnan Li, Dongxu Li, Silvio Savarese, and Steven C. H. Hoi. BLIP-2: bootstrapping language-image pre-training with frozen image encoders and large language models. In *ICML*, pages 19730–19742. PMLR, 2023. 2
- [15] Junnan Li, Dongxu Li, Silvio Savarese, and Steven C. H. Hoi. BLIP-2: bootstrapping language-image pre-training with frozen image encoders and large language models. In *ICML*, pages 19730–19742. PMLR, 2023. 1
- [16] Xiang Li, Like Li, Yuchen Jiang, Hao Wang, Xinyu Qiao, Ting Feng, Hao Luo, and Yong Zhao. Vision-language models in medical image analysis: From simple fusion to general large models. *Inf. Fusion*, 118:102995, 2025. 1
- [17] Haotian Liu, Chunyuan Li, Qingyang Wu, and Yong Jae Lee. Visual instruction tuning. In *NeurIPS*, 2023. 2
- [18] Haotian Liu, Chunyuan Li, Qingyang Wu, and Yong Jae Lee. Visual instruction tuning. In *NeurIPS*, 2023. 1
- [19] Haotian Liu, Chunyuan Li, Yuheng Li, and Yong Jae Lee. Improved baselines with visual instruction tuning. In *CVPR*, pages 26286–26296. IEEE, 2024. 2
- [20] Haotian Liu, Chunyuan Li, Yuheng Li, and Yong Jae Lee. Improved baselines with visual instruction tuning. In *CVPR*, pages 26286–26296. IEEE, 2024. 1, 6
- [21] Haotian Liu, Chunyuan Li, Yuheng Li, Bo Li, Yuanhan Zhang, Sheng Shen, and Yong Jae Lee. Llava-next: Improved reasoning, ocr, and world knowledge, 2024. 1, 2, 7, 8
- [22] Tharindu Madusanka, Iqra Zahid, Hao Li, Ian Pratt-Hartmann, and Riza Batista-Navarro. Not all quantifiers are equal: Probing transformer-based language models’ understanding of generalised quantifiers. In *EMNLP*, pages 8680–8692. Association for Computational Linguistics, 2023. 1
- [23] Noorul Husna Abd Rahman, Ayman Khallel Ibrahim, Khairunnisa Hasikin, and Nasrul Anuar Abd Razak. Critical device reliability assessment in healthcare services. *Journal of Healthcare Engineering*, 2023, 2023. 2
- [24] Javier Rodríguez-Juan, David Ortiz-Perez, José García Rodríguez, David Tomás, and Grzegorz J. Nalepa. Integrating advanced vision-language models for context recognition in risks assessment. *Neurocomputing*, 618:129131, 2025. 1
- [25] Yuzhang Shang, Mu Cai, Bingxin Xu, Yong Jae Lee, and Yan Yan. Llava-prumerge: Adaptive token reduction for efficient large multimodal models. *CoRR*, abs/2403.15388, 2024. 1, 2, 5, 6
- [26] Dachuan Shi, Chaofan Tao, Anyi Rao, Zhendong Yang, Chun Yuan, and Jiaqi Wang. Crossget: Cross-guided ensemble of tokens for accelerating vision-language transformers. In *ICML*. OpenReview.net, 2024. 1
- [27] Amanpreet Singh, Vivek Natarajan, Meet Shah, Yu Jiang, Xinlei Chen, Dhruv Batra, Devi Parikh, and Marcus Rohrbach. Towards VQA models that can read. In *CVPR*, pages 8317–8326. Computer Vision Foundation / IEEE, 2019. 2, 5
- [28] Dingjie Song, Wenjun Wang, Shunian Chen, Xidong Wang, Michael X. Guan, and Benyou Wang. Less is more: A simple yet effective token reduction method for efficient multimodal llms. In *COLING*, pages 7614–7623. Association for Computational Linguistics, 2025. 1, 2, 6
- [29] Yizheng Sun, Hao Li, Chenghua Lin, and Riza Batista-Navarro. Lanvikd: Cross-modal language-vision knowledge distillation for egocentric action recognition. In *HAI15.0@ECAI*. CEUR-WS.org, 2024. 1
- [30] Yizheng Sun, Yanze Xin, Hao Li, Jingyuan Sun, Chenghua Lin, and Riza Batista-Navarro. Lvpruning: An effective yet simple language-guided vision token pruning approach for multi-modal large language models. *CoRR*, abs/2501.13652, 2025. 1

- [31] An Yang, Baosong Yang, Binyuan Hui, Bo Zheng, Bowen Yu, Chang Zhou, Chengpeng Li, Chengyuan Li, Dayiheng Liu, Fei Huang, Guanting Dong, Haoran Wei, Huan Lin, Jialong Tang, Jialin Wang, Jian Yang, Jianhong Tu, Jianwei Zhang, Jianxin Ma, Jianxin Yang, Jin Xu, Jingren Zhou, Jinze Bai, Jinteng He, Junyang Lin, Kai Dang, Keming Lu, Keqin Chen, Kexin Yang, Mei Li, Mingfeng Xue, Na Ni, Pei Zhang, Peng Wang, Ru Peng, Rui Men, Ruize Gao, Runji Lin, Shijie Wang, Shuai Bai, Sinan Tan, Tianhang Zhu, Tianhao Li, Tianyu Liu, Wenbin Ge, Xiaodong Deng, Xiaohuan Zhou, Xingzhang Ren, Xinyu Zhang, Xipin Wei, Xuancheng Ren, Xuejing Liu, Yang Fan, Yang Yao, Yichang Zhang, Yu Wan, Yunfei Chu, Yuqiong Liu, Zeyu Cui, Zhenru Zhang, Zhifang Guo, and Zhihao Fan. Qwen2 technical report. *CoRR*, abs/2407.10671, 2024. [1](#)
- [32] Senqiao Yang, Yukang Chen, Zhuotao Tian, Chengyao Wang, Jingyao Li, Bei Yu, and Jiaya Jia. Visionzip: Longer is better but not necessary in vision language models. *CoRR*, abs/2412.04467, 2024. [1](#), [2](#), [6](#)
- [33] Yue Zheng, Yuhao Chen, Bin Qian, Xiufang Shi, Yuanchao Shu, and Jiming Chen. A review on edge large language models: Design, execution, and applications. *CoRR*, abs/2410.11845, 2024. [1](#)
- [34] Beier Zhu and Hanwang Zhang. Debiasing vision-language models for vision tasks: a survey. *Frontiers Comput. Sci.*, 19(1):191321, 2025. [6](#)